Dental Materials xxx (xxxx) xxx–xxx

Contents lists available at ScienceDirect

Dental Materials

journal homepage: www.elsevier.com/locate/dental

Development, characterization and antimicrobial activity of multilayer silica nanoparticles with chlorhexidine incorporated into dental composites

Pavanello Larissa[a], Benjamin Gambrill[b], Rafaela Durrer Parolina de Carvalho[a], Mayara Zagui Dal Picolo[a], Vanessa Cavalli[a], Letícia Cristina Cidreira Boaro[c], Polina Prokopovich[b,1,*], Karina Cogo-Müller[d,1]

[a] Piracicaba Dental School, University of Campinas, Piracicaba, SP, Brazil
[b] School of Pharmacy and Pharmaceutical Science, Cardiff University, Cardiff, United Kingdom
[c] Santo Amaro University, Dental School, São Paulo, Brazil
[d] Faculty of Pharmaceutical Sciences, University of Campinas, Campinas, Brazil

ARTICLE INFO

Keywords:
Silica
Chlorhexidine
Dental composites
LbL

ABSTRACT

Objective: In this study a dentistry nanocomposite with prolonged antibacterial activity using silica nanoparticles (SNPs) loaded with chlorhexidine (CHX) was developed.
Methods: SNPs were coated with the Layer-by-Layer technique. Dental composites were prepared with organic matrix of BisGMA/TEGDMA and SNPs with or without CHX (0, 10, 20 or 30% w/w). The physicochemical properties of the developed material were evaluated and agar diffusion method was used to test the antibacterial. In addition, the biofilm inhibitory activity of the composites was evaluated against *S. mutans*.
Results: SNPs were rounded with diameters about 50 nm, the organic load increased with increasing deposited layers. Material samples with SNPs loaded with CHX (CHX-SNPs) showed the highest values of post-gel volumetric shrinkage, that ranged from 0.3% to 0.81%. Samples containing CHX-SNPs 30% w/w showed the highest values of flexural strength and modulus of elasticity. Only samples containing SNPs-CHX showed growth inhibition against *S. mutans, S. mitis and S. gordonii* in a concentration-dependent manner. The composites with CHX-SNPs reduced the biofilm formation of *S. mutans* biofilm at 24 h and 72 h.
Significance: The nanoparticle studied acted as fillers and did not interfere with the evaluated physicochemical properties while providing antimicrobial activity against streptococci. Therefore, this initial study is a step forward to the synthesis of experimental composites with improved performance using CHX-SNPs.

1. Introduction

Different types of nanoparticles (NPs) have been added to dental composites, such as silica NPs (SNPs), to optimize optical, physical-chemical and mechanical properties, morpho-physiology and dental esthetics, in addition to obtaining therapeutic effects through nanocarriers and sustained release of active substances at the target local [1].

Considering the possibility of failures and the need to replace composite resins, the complexity and dynamism of the oral microbiome, as well as the negative impact of dysbiosis in restorative dental procedures, the association of nanocomposites with antimicrobial agents is a viable prophylactic alternative for recurrent oral infectious complications [2–4]. Several antimicrobials have been extensively studied and tested in dental nanocomposites. Among these, the use of chlorhexidine (CHX), a broad-spectrum bisbiguanide antiseptic widely used in clinical dental practice for the prevention and treatment of oral infections, has been explored [5,6]; recently also application in orthopedic have been reported [7]. It is expected that CHX-associated nanocomposites present a sustained release profile at the tooth/nanocomposite interface, reducing bacterial adhesion on the experimental composite without affecting the homeostasis and viability of oral cells

* Correspondence to: School of Pharmacy and Pharmaceutical Sciences, Cardiff University, Redwood Building, King Edward VII Avenue, Cardiff CF10 3NB, United Kingdom.
E-mail address: prokopovichp@cf.ac.uk (P. Prokopovich).
[1] Karina Cogo-Müller and Polina Prokopovich are both senior authors and contributed equally.

https://doi.org/10.1016/j.dental.2023.03.005
Received 31 October 2022; Received in revised form 12 February 2023; Accepted 3 March 2023

[3]. Current antimicrobial releasing dental nanocomposites do not exhibit an optimal release profile with an initial burst followed by a quick drop in the drug release rate; this results in short acting antimicrobial properties.

The layer-by-layer technique (LbL) has great potential in the sustained/controlled delivery of drugs, by creating multiple nanostructures that act as a drug reservoir [7–11]. Recent studies investigated the incorporation of gentamicin-loaded SNPs and CHX-loaded-SNPs synthesized by the LbL technique into polymethylmethacrylate (PMMA) bone cements for prophylaxis of prosthetic joint infections (PJI) [7,8,10]. The antimicrobial releasing SNP showed prolonged and superior antimicrobial activity than the free drug, cytocompatibility, good diffusivity and preservation of the properties of the bone cements tested. One of the main features related to these SNPs is the use of poly-beta-amino-esters (PBAEs), a weakly positively charged and hydrolysable polymer, in the construction of the coatings on the SNPs surfaces. These polymers are synthesized with amines and di-acrylates and are highly biocompatible [7–11].

Aiming at the development of a restorative nanomaterial with antimicrobial activity and improved mechanical properties, a dental nanocomposite material containing CHX-loaded SNPs (CHX-SNPs) synthesized by LbL was developed and characterized. the impact of the incorporation of CHX-SNPs on the physicochemical properties of the dental nanocomposite and the antimicrobial activity of the CHX-SNPs containing material were tested.

2. Materials and methods

2.1. Synthesis and characterization of PBAE

3.7 mmol of Bisphenol A ethoxylate diacrylate with a 4.1 mmol of piperazine (Fig. 1) were mixed in 5 mL of dichloro methane (DCM). The polymer synthesis was performed under stirring at 50 °C for 48 h. Amino terminated PBAEs were recovered by precipitated in about 50 mL of diethyl ether followed by solvent evaporation under vacuum [8,10].

The reaction products were analyzed through GPC and NMR [8,10].

2.2. Synthesis and characterization of CHX-loaded SNPs (CHX-SNPs)

SNPs were prepared by the Stöber method [12] based on the hydrolysis of TEOS in reverse microemulsion and subsequent surface functionalization with amine groups by adding APTS to the micro-emulsion under agitation and incubation for further 24 h.

Triton X-100 (17.7 g), n-hexanol (16 mL), cyclohexane (75 mL) and 4.8 mL of deionised water were mixed under stirring until the solution was transparent; 600 µL of NH_4OH (29.6%) were added. 1 mL of TEOS was added with stirring continued for further 24 h when 50 µL of APTS were added; the micro-emulsion was stirred for further 24 h.

SNPs were recovered by adding ethanol and centrifuging at 14,000 rpm for 10 min (LE-80 K, Ultracentrifuge, Beckman Coulter, UK) at 20 °C (35,280 g). The SNPs were washed three times with deionized water and left to dry at room temperature in a fume hood for 24 h. Then, the SNPs were layered with a repeated sequence of alginate, PBAE and CHX diacetate (10% w/w) resulting in a total of 40 layers corresponding to 10 quadruple layers of the main unit (alginate-CHX-alginate-PBAE) [7,8].

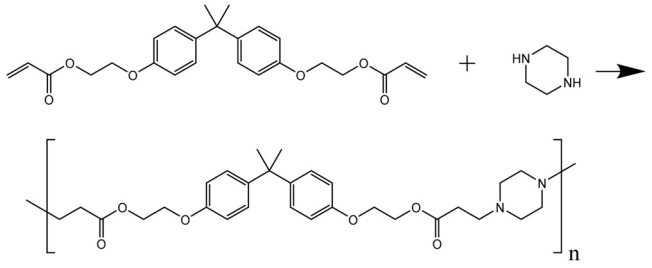

Fig. 1. Scheme of reaction for the synthesis of PBAE.

The size of the CHX-SNPs was characterized by transmission electron microscopy (TEM, JEOL-1010 microscope). TEM images were analyzed with ImageJ® software and the diameters of at least 150 particles were measured. Electrophoretic mobility of the polyelectrolytes was measured by dynamic light scattering (DLS), using Malvern Zetasizer, Nano ZS particle (Malvern Instruments Limited, UK). The measured electrophoretic mobility was converted to zeta potential values (ζ) using the Smoluchowski model. Thermal gravimetry analysis (TGA) was performed using a Perkin-Elmer TGA 4000 instrument. During constant heating, the sample weight was recorded and weight loss percentage of each sample was calculated relative to initial weight of sample, prior to heating [7,8].

CHX release from CHX-SNPs (10 mg) was evaluated by dispersing the NPs in 1 mL of two buffer media (acetic acid-sodium acetate buffer - pH 5 and PBS - pH 7.3). After vigorous shaking and incubation at 37 °C; every 24 h particles were centrifuged at 14,000 rpm for 10 min and the supernatant was collected for quantification of released CHX. The particles were resuspended in 1 mL of fresh buffer medium and incubated at 37 °C.

CHX quantification was performed using reversed-phase High Performance Liquid Chromatography (HPLC) method (Agilent Technologies® 1100 series HPLC). Standard concentrations were prepared by serial dilutions of a CHX stock solution (1 mg/mL) to a range of 0.4–25 µg/mL. Each data point is an average of three replicates [7,8].

2.3. Dental composites preparation

Seven experimental composites groups were prepared, using resin matrices based on Bis-GMA (Bisphenol A Bis (2-hydroxy-3-methacryloxypropyl) Ether, Esstech, Essington, Pennsylvania, USA) and TEGDMA (Triethyleneglycol Dimethacrylate, Esstech,) in equal weight proportions. The photoinitiator system used was composed of 1% (w/w) DMAEMA (2-(dimethylamino) ethyl methacrylate - 98%, Sigma-Aldrich, Steinheim, Germany) and 0.8% (w/w) camphorquinone (97%, Sigma-Aldrich, Steinheim, Germany) [3]. CHX loaded SNPs and pure SNP were added to the composites in proportions of 0 (control group), 10, 20, or 30% (w/w), in a dark room with yellow lighting to avoid polymerization during the manufacturing process, with mixing for 3 min using an automatic vacuum mixer (SpeedMixer DAC 150 FVZ, Hauschild) at 3500 rpm. Similarly, pure CHX was mixed in added to the monomers in quantities equivalent to the amount of CHX added when deposited on the SNP.

The samples were light-cured on top for 40 s, using an LED device (VALO Cordless, Ultradent Products Inc., South Jordan, UT, USA) operating in a standard mode (1000 mW/cm^2), between two glass slides in a silicone mold. The specimens were made 24 h before use and were stored dry at 37 °C in hermetically closed dark flasks until the time of use. Two types of molds were used for specimen production, bar-shaped for the flexural strength test (10 mm × 2 mm × 1 mm) [13] and disk-shaped (7 mm × 1 mm) [3] for the remaining assays.

2.4. Degree of conversion (DC)

Fourier transform infrared (FTIR - Vertex 70, Bruker Optik GmbH, Alemanha) spectroscopy was utilized for DC analysis. Sample were placed into the FTIR spectrophotometer so that the laser beam passed through the center of the specimen. Spectra were recorded from the uncured composites and immediately after photopolymerization. The area under the peak 6165 cm^{-1}, corresponding to the vinyl bond, was obtained [3,14]. DC was calculated as a function of the area of the vinyl peak (DC = (1 – polymerized / not polimerized) × 100%). Results are presented as the average ± SD of 3 independent samples.

2.5. Chlorohexidine release from dental cement

Disk-shaped samples were incubated in 1 mL PBS buffer (pH 7.4) at 37ºC. The buffer was replaced each day (sink condition) and the concentration of released chlorhexidine determined through HPLC. The specimens were stored in a refrigerator (2–8 ºC) for no more than 3 d prior to analysis. CHX released is expressed as % of the initial CHX amount in the samples based on the CHX loading in the SNP-CHX and the amount of SNP mixed in the dental material. Resulted are presented as the average ± SD of 3 independent samples.

2.6. Evaluation of the mechanical properties

2.6.1. Flexural strength (FS) and flexural modulus (FM)

FS and FM were evaluated after 24 h of photoactivation and 60 days of immersion in distilled water and stored in an incubator (Tecnal TE – 392/2, São Paulo, Brazil) at 37 °C. The specimens were submitted to a three-point flexure device using a universal testing machine (Instron, 5565, Canton, MA, USA) with 8 mm distance between supports and crosshead speed of 0.5 mm/min until failure.

The maximal FS was calculated according to the following equation:

$$\sigma = \frac{3FL}{2bh^2}$$

where σ is the flexural strength (MPa), F is the maximum load recorded before the specimen fractured (N), L is the distance between the supports (mm), b is the width of the specimen (mm), and h is the height of the specimen (mm), respectively and FM was calculated as:

$$E = \frac{CL^3}{4bh^3D}10^{-3}$$

where E is the flexural modulus (GPa), C is the load recorded (N), L is the span between the supports (mm), b is the width of the specimen (mm), h is the height of the specimen (mm) and D is the deflection corresponding to C (mm).

Results are presented as average ± SD of 10 independent sample.

2.6.2. Post-gel volumetric shrinkage

Post-gel volumetric shrinkage was measured using the biaxial "strain gage" method [15,16]. Approximately 0.1 g of sample were placed on a unidirectional strain gauge (PA-06–060BG-350LEN Excel, São Paulo, Brazil) connected to an adapter for Instron and a microcomputer; signals from the data acquisition board were recorded through BlueHill software. Samples were light-activated under the same conditions described above and the contraction was monitored for 5 min from photoactivation. Deformation resulting from material contraction was measured in two perpendicular directions.

2.6.3. Surface roughness

Surface roughness (Ra) was evaluated dry storage 24 h after photoactivation by a surface tester (Mitutoyo Surftest SJ-410, São Paulo, Brazil). Three measurements were performed on each specimen by rotating the specimen 45°, with a cut-off at 0.8 mm and speed of 0.5 mm/s. Results are presented as average ± SD of 10 independent sample.

2.7. Evaluation of antimicrobial properties

2.7.1. Bacterial sensitivity test by agar diffusion technique

The agar dilution method was performed according to Clinical Standard Laboratory Institute M2-A8 protocol (CLSI, 2003) using three bacterial strains *Streptococcus mutans* (UA 159), *Streptococcus mitis* (ATCC 49456) and *Streptococcus gordonii* (ATCC 35105).

Overnight cultures were grown using 30 µL of the frozen stocks in glass tubes containing 9 mL of BHI (Brain Heart Infusion Broth, Kasvi, Laboratorios Conda S.A, Madrid, Spain) broth. The cultures were incubated (Sanyo Eletric Co., Japan, MCO-19AIC) for 24 h in an 10% CO_2 atmosphere at 37 °C. To prepare the bacterial inoculum, 300 µL of the overnight mixture was suspended in a glass tube containing 5 mL of 0.9% saline solution, to reach the density equivalent to the turbidity of the 0.5 McFarland standard solution (wavelength = 625 nm) (CLSI, 2003).

The bacterial suspension was spread over the agar surface Müeller-Hinton agar (HiMedia Laboratories Pvt.Ltd, Mumbai, India) supplemented with 5% sheep blood (Anilab Animais para Pesquisa Criação e Comérico – LTDA, Paulínia, São Paulo) using a sterile swab. Specimens (n = 5) were disinfected with a gauze soaked in 70° alcohol (5 strokes coming and going by surface) and UV light irradiation for 1 min (mercury vapor lamp with > 90% radiation at 253.7 nm) on both sides. Then, the specimens were positioned over the agar and the plates were incubated for 24 h, at 37 °C, in a 10% CO_2 atmosphere. After this period, the total inhibition zones diameter were measured using a digital caliper, disregarding the size of the specimen [17].

2.7.2. Monospecies biofilm inhibition assay

The biofilm assay was adapted from methods described previously [18,19]. *S. mutans* inoculum was prepared by transferring 30 µL of the frozen stock to a glass tube containing 9 mL of BHI broth, followed by incubation for 18 h, at 37 °C, in a 10% CO_2 atmosphere. The optical density was adjusted to approximately 0.7, at a wavelength of 660 nm.

Previously sterilized specimens (n = 6, under the same conditions described above) were embedded in metallic apparatus, and placed in the 24-well polystyrene plates, in vertical position. Each well received 2.85 mL of BHI broth, 0.15 mL of 20% sucrose solution, and 12 µL of bacterial inoculum. To control for experimental contamination, groups containing only the specimens and culture medium were also tested (n = 2). The plates were incubated for 24 or 72 h, at 37 °C, in a 10% CO_2, and culture medium was renewed daily (for the 72 h-biofilm). After the incubation periods (24 h or 72 h), discs were removed, washed, and prepared, in order to determine viable cells by the plating method. To remove non-adherent bacterial cells, the biofilms were gently washed (1x) in a 24-well plate with 3 mL of 0.9% sterile saline. Subsequently, the discs were transferred to polystyrene tubes containing 5 mL of sterile saline, vortexed for 1 min, and sonicated for 1 min (5% amplitude, 6 pulses, 9.9 s for each pulse, and 5 s intervals), at 4 °C (Vibra-Cell VCX400 sonicator, Sonics, USA). Serial dilutions from this suspension were plated on BHI agar. The plates were incubated for 48 h, followed by counting of the colonies to obtain the number of colony forming units per mL (CFU/mL). The experiments were performed in duplicate.

2.8. Statistical analysis

Data were plotted with R software [20]. The degree of conversion, post-gel volumetric shrinkage, surface roughness and inhibition zone results were analyzed by one-way analysis of variance (ANOVA) followed by Tukey's multiple comparison test was performed with SPSS (SPSS Inc., version 21.0; Chicago, USA). Monospecies biofilm inhibition, flexural strength, and flexural modulus results were analyzed by two-way ANOVA followed by Tukey's multiple comparison test according to normality and homoscedasticity conditions. For variables evaluated before and after storage, Student's "t" test was used. The significance level was set at 5%.

3. Results

3.1. Characterization of SNPs-loaded chlorhexidine (CHX-SNPs)

3.1.1. Particle size

The synthesized SNPs had a circular shape with diameters normally distributed (Fig. 2); the uncoated SNPs had a mean diameter of 58 nm (sd = 13 nm). After the deposition of 10 quadruple layers containing CHX, SNPs had a mean diameter of 69 nm (SD = 9 nm).

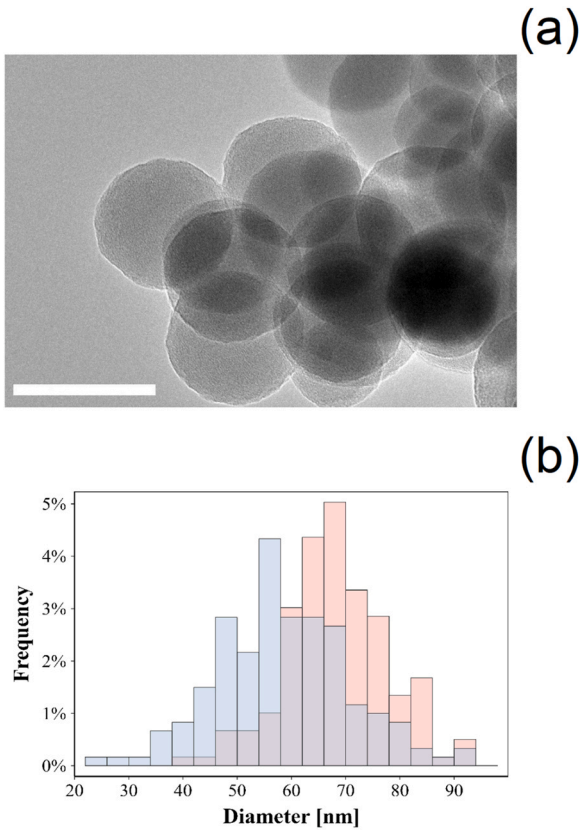

Fig. 2. Example of TEM image (bar represent 50 nm) of uncoated SNPs (a) and diameter distribution of uncoated SNPs ( ) and after deposition of 10 QL ( ) (b).

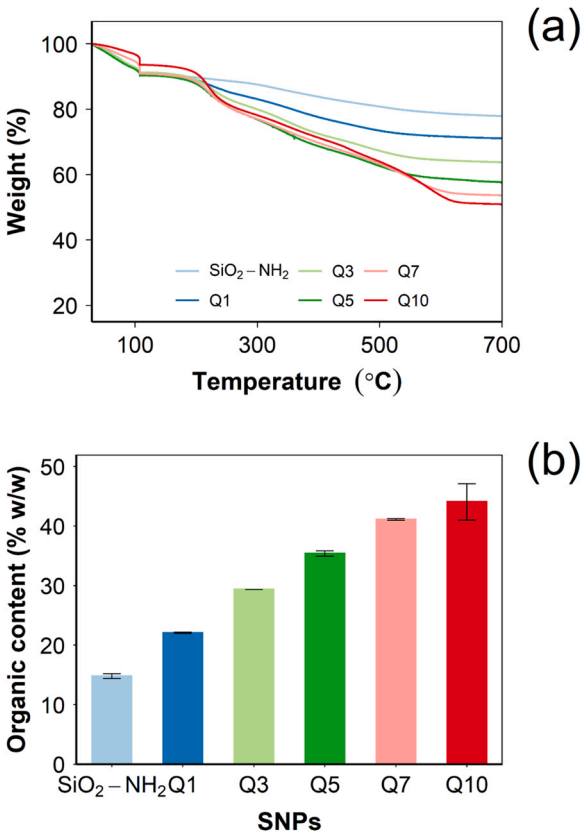

Fig. 3. Example of thermograms of SNP after deposition of different numbers of quadruple layers containing CHX (a); organic content of SNPs after deposition of different numbers of quadruple layers containing CHX determined through TGA (mean ± SD, n = 3) (b).

3.1.2. Zeta potential

Uncoated SNPs had a positive charge exhibiting a zeta potential of 23.73 mV; after the deposition of alginate the charge on the SNPs was reversed and the zeta potential was − 30.30 mV. The subsequent deposition of CHX resulted in a further charge swap with a zeta potential of 25.03 mV; finally, the last step of the quadruple layer formation (deposition of PBAE) resulted in a moderate positive charge with zeta potential of 2.73 mV (Table 1).

3.1.3. Thermogravimetric analysis (TGA)

When heated the SNP exhibited a progressive weight loss with a particular jump at around 100 °C reaching a plateau at temperatures above 650 °C (Fig. 3a); this represents the amount of organic content in the SNPs. The greater the number of deposited quadruple layers the greater the total weight loss when reaching the plateau. The uncoated SNPs had about 12% w/w of organic content, the deposition of multiple quadruple layers containing CHX resulted in greater organic fraction, after 10 quadruple layers, the SNPs exhibited about 45% of organic materials (Fig. 3b).

Table 1
Zeta potential of uncoated SNPs (SiO_2-NH_2) and during deposition of one quadruple layer.

SNPs	Zeta potential [mV] (mean ± SD, n = 3)
SiO_2-NH_2	23.73 ± 0.65
SiO_2-NH_2-Alg	-30.30 ± 2.79
SiO_2-NH_2-Alg-CHX	25.03 ± 0.96
SiO_2-NH_2-Alg-CHX-Alg	-31.80 ± 1.15
SiO_2-NH_2-Alg-CHX-Alg-PBAE	2.73 ± 0.52

3.1.4. CHX release quantification

SNPs released the CHX present in the coatings when in contact with aqueous solutions; the release rate was pH dependent with higher release at pH = 7.4 then pH = 5 (Fig. 3). In acidic conditions the released completed after about 60 days while at pH = 7.4, no more CHX was detected in the release buffer after about 45 days. Overall, the amount of CHX released was greater at pH = 7.4 than pH = 5.

3.2. Evaluation of the dental composites properties

3.2.1. Degree of conversion

Degree of conversion ranged from 69.3% (20% SNPs) to 76.3% (30% SNPs and 20% CHX-SNPs) (Table 2). No significant differences were found among the groups ($p > 0.05$, Table 2).

3.2.2. Post-gel volumetric shrinkage

Post-gel volumetric shrinkage values ranged from 0.3 (10% SNPs) to 0.71% (10% CHX-SNPs) (Table 2). In general, the CHX-SNPs groups showed higher values, comparing to control and plain SNPs ($p < 0.05$). Differences were found between the SNPs and CHX-SNPs groups, when comparing the same concentrations ($p < 0.05$), except for the 30% group. The control group differed statistically ($p < 0.05$) from the 10% and 20% CHX-SNPs groups, which exhibited higher post-gel volumetric shrinkage.

3.2.3. Surface roughness

The surface roughness of the experimental composites gradually increased with increasing percentages of SNPs and CHX-SNPs ($p < 0.05$, Table 2), with values ranging from 0.018 (10% SNPs and 10% CHX-SNPs) to 0.038 μm (30% CHX-SNPs). There was no statistical difference between SNPs and CHX-SNPs groups, when comparing the

Table 2
Means and standard deviations for degree of conversion (n = 3), post-gel volumetric shrinkage (n = 5) and surface roughness (n = 10).

Groups	Degree of conversion (%)	Post-gel volumetric shrinkage (%)	Surface roughness (μm)
Control	73.4 ± 0.51 a	0.390 ± 0.0 BCE	0.023 ± 0.008 bcd
CHX-SNPs 10%	73.1 ± 4.91 a	0.714 ± 0.24 a	0.018 ± 0.002 cd
CHX-SNPs 20%	76.3 ± 4.26 a	0.696 ± 0.13 a	0.030 ± 0.007 ab
CHX-SNPs 30%	72.3 ± 0.45 a	0.570 ± 0.05 ab	0.038 ± 0.01 a
SNPs 10%	72.5 ± 1.21 a	0.3 ± 0.04c	0.018 ± 0.005 d
SNPs 20%	69.3 ± 1.98 a	0.306 ± 0.11 BCE	0.028 ± 0.006 BCE
SNPs 30%	76.3 ± 3.27 a	0.402 ± 0.13 bc	0.032 ± 0.008 ab

Means values followed by the same superscript letters are statistically similar ($p < 0.05$ – One-way ANOVA/Tukey).

Table 3
Means and deviations for flexural strength (MPa) and flexural modulus (GPa) after 24 h of polymerization ($n = 10$) and after 60 days immersion in distilled water ($n = 10$).

	After 24 h of polymerization		After 60 days immersed in distilled water	
Groups	Flexural strength (mean ± SD)	Flexural modulus (mean ± SD)	Flexural strength (mean ± SD)	Flexural modulus (mean ± SD)
Control	29.96 ± 4.92 bcB	0.339 ± 0.09 cB	35.89 ± 2.21 aA	0.527 ± 0.07 cdA
CHX-SNPs 10%	31.29 ± 5.08 abcA	0.395 ± 0.12 bcB	33.35 ± 3.66 abA	0.647 ± 0.08 abA
CHX-SNPs 20%	34.4 ± 6.15 abA	0.474 ± 0.37 bcA	30.38 ± 3.04 bcdA	0.614 ± 0.07 abcA
CHX-SNPs 30%	37.39 ± 5.56 aB	0.702 ± 0.13 aA	30.67 ± 2.69 bcA	0.688 ± 0.11 aA
SNPs 10%	26.72 ± 6.02 cA	0.463 ± 0.13 BCEA	28.37 ± 4.76 cdA	0.271 ± 0.14 eB
SNPs 20%	31.64 ± 4.49 abcA	0.481 ± 0.17 bcA	30.62 ± 3.08 bcA	0.559 ± 0.07 bcA
SNPs 30%	30.18 ± 4.43 bcA	0.555 ± 0.07 abA	26.64 ± 2.68 dA	0.439 ± 0.09 dA

Means values followed by the same superscript letters were statistically similar ($p < 0.05$ – One-way ANOVA/Tukey). Lowercase letters represent analysis between groups in each time evaluated. Capital letters represent the comparison between groups at different times.

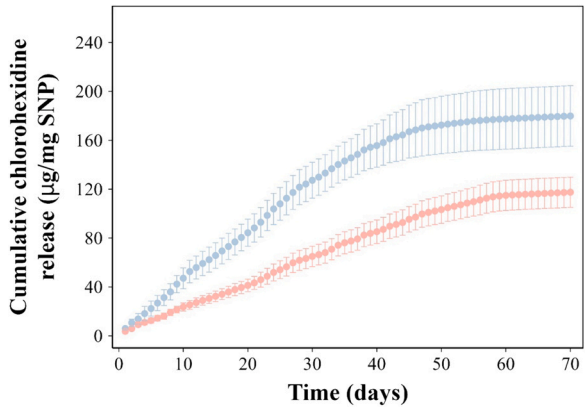

Fig. 4. Release profile of CHX from SNPs coated with 10 quadruple layers at pH = 5 ( ) and pH = 7.4 ( ) (mean ± SD, n = 3).

same concentrations ($p > 0.05$). The control group differed statistically ($p < 0.05$) only for the 30% CHX-SNPs group, which exhibited higher surface roughness.

3.2.4. Flexural strength and flexural modulus

The means and standard deviations (SD) for flexural strengths (GPa) and flexural modulus (MPa) are shown in Table 3 for the two times of analysis.

For flexural strength, the CHX-SNPs group showed higher values, compared to the control and SNPs groups, 24 h after polymerization. The highest flexural strength was obtained for the 30% CHX-SNPs group, which was the only group statistically different from the control ($p < 0.05$). Comparing the same concentrations for the groups with and without CHX, a significant difference was only observed for the groups with 30% of NPs ($p < 0.05$). The storage time in water was significant for the control and 10% CHX-SNPs groups ($p < 0.05$). After storage, these groups showed higher flexural strength, compared to the other groups. When comparing the same concentrations, a significant difference was observed for the groups with 10% and 30% NPs ($p < 0.05$).

In general, for the flexural modulus, the 30% CHX-SNPs group showed the highest values ($p < 0.05$), for both times of analysis. At 24 h after polymerization, no difference was found between the SNPs and CHX-SNPs groups, when comparing the same concentrations ($p > 0.05$), and at 30% both groups differed statistically from the control. On the other hand, after storage in distilled water, there was a statistical difference ($p < 0.05$) when comparing the same concentrations, except for the 20% group. The 10% and 30% CHX-SNPs groups differed significantly from the control group. The storage time was significant for the control, 10% CHX-SNPs, and 10% SNPs groups ($p < 0.05$).

3.3. CHX release

CHX release from dental composites containing CHX-SNPs exhibited a similar pattern then from directly SNPs, with a rate decreasing with time (Fig. 5). The impact of pH conditions on the release was detectable only in the dental materials containing the lowest amount of SNPs (10% w/w). The rate of CHX release from the dental sample decreased with increasing CHX-SNPs; after 30 days, about 12% of the CHX contained in the added SNPs was released from samples prepared with 10% w/w of CHX-SNPs while only 5% and 3% of the initial drug amount was released after the same time from samples prepared with 20% and 30% w/w CHX-SNPs, respectively. When the same amount of CHX was added to the dental materials, the release of CHX was faster and completed after about 1 week regardless of the pH.

3.4. Antimicrobial properties of dental composites

3.4.1. Bacterial sensitivity test by agar diffusion method

Antimicrobial activity of CHX-SNPs/experimental composites was tested through agar dilution method against strains of *S. mutans*, *S. mitis* and *S. gordonii*. The results (Fig. 6) showed that the CHX-SNPs groups formed inhibition zones for all the bacteria, with the 30% CHX-SNPs group presenting higher antimicrobial activity, compared to the other concentrations ($p < 0.05$). No inhibition zones were observed for SNPs and control groups.

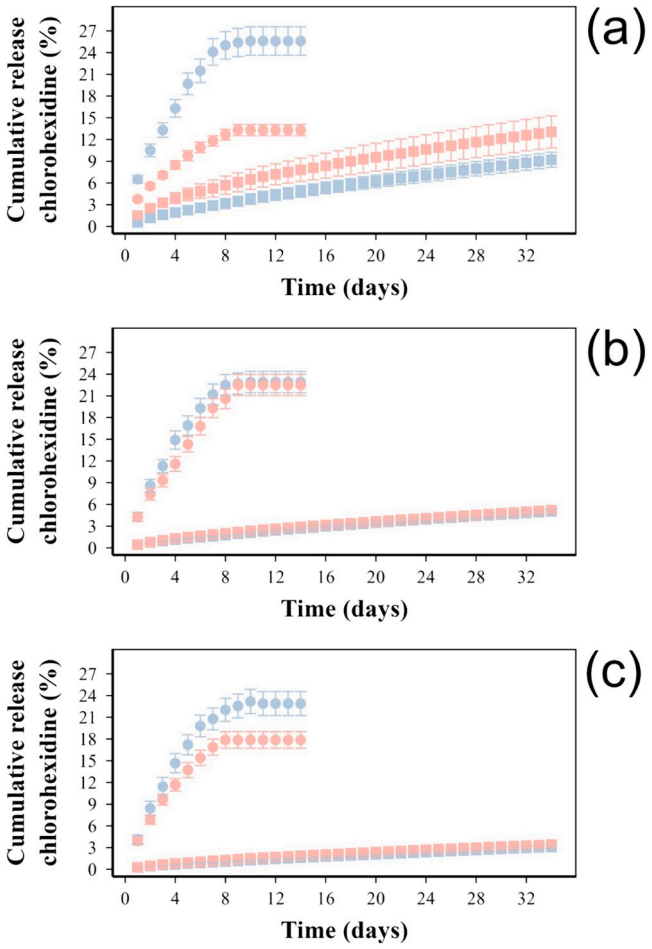

Fig. 5. Cumulative release of CHX from dental composite (as % of the initial CHX loaded in the samples) with 10% w/w (a), 20% w/w (b) or 30% w/w (c) CHX-SNPs at pH = 5 ( ) and pH = 7.4 ( ) from dental material containing CHX-SNPs (squares) or pure CHX (circles) (mean ± SD, n = 3).

For *S. mutans* biofilm, the number of colony forming units per mL (CFU/mL) was reduced with CHX-SNPs incorporated in the experimental composites, both after 24 h and 72 h (Fig. 7). When comparing CHX-SNPs groups, after both exposure times, CHX-SNPs 30% returned the highest CFU/mL reduction ($p < 0,05$). Significant differences ($p < 0,05$) were also found between SNPs and CHX-SNPs groups when comparing the same samples with the same SNPs concentrations. After 24 h, experimental composites with 20% and 30% w/w of SNPs were statistically different ($p < 0,05$), while after 72 h only the highest SNPs concentration showed a significant difference ($p < 0,05$). The time of biofilm formation significantly influenced the results for the 20% and 30% CHX-SNPs groups.

4. Discussion

The appearance of marginal cracks at the tooth/restoration interface and, consequently, recurrent episodes of caries, are the main factors that negatively affect the long-term clinical performance of composite resin restorations. These factors are primarily related to the properties presented such materials, especially the physicochemical properties [18,19]. In order to overcome these limitations and considering the reinforcing effect of SNPs, as well as the broad-spectrum antimicrobial activity of CHX, an experimental composite containing CHX-SNPs in different concentrations was developed and its general performance evaluated.

The SNPs developed here had similar properties to other silica-based drug releasing systems in terms of size (Fig. 2); moreover, the increased size after deposition was also expected as consequence of the adhering layers [7–9]. The successful deposition of the desired layer was also confirmed by see-saw profile of the zeta potential after each deposited layer (Table 1) and the TGA analysis (Fig. 3) resulting in similar drug loads as using other PBAEs [7–9]. These are a class of polymers that are positively charged, hydrolysable and highly biocompatible [20]. They were initially employed as DNA non-viral delivery vector [21,22]; nevertheless, they have found also wide application in the development of functional coatings as one the polyelectrolytes used in LbL [7–10,23–25]. Drug release from coatings prepared with PBAEs generally is controlled by the active molecule diffusion through the deposited layers more than by the hydrolyzation of the polymers. This results in higher release kinetics in neutral conditions, where the drug diffusion coefficient is higher in light of the reduced PBAE charge, than in acidic environments, where, despite a faster PBAEs hydrolysis, the higher PBAE positive charge reduces the drug diffusion coefficient [11]. The drug release profiles observed in this work (Fig. 4) further confirm the assumed mechanisms underlaying the drug release process and their governing factors [7–10]. Furthermore, the results support the use of coated SNPs to sustain and prolong the release of active compounds such as chlorhexidine from dental materials.

The results obtained for the degree of conversion (Table 2) were satisfactory and showed that there was no difference in polymerization

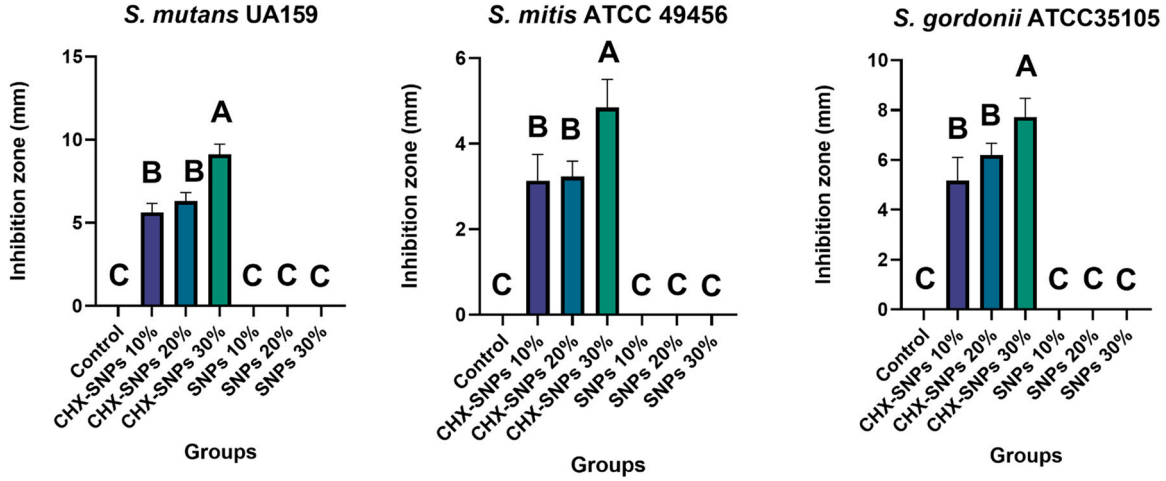

Fig. 6. Means and standard deviation values calculated for the agar dilution method. Means values followed by the same letter were statistically similar ($p > 0.05$, one-way ANOVA/Tukey).3.4.2 Monospecies biofilm inhibition assay.

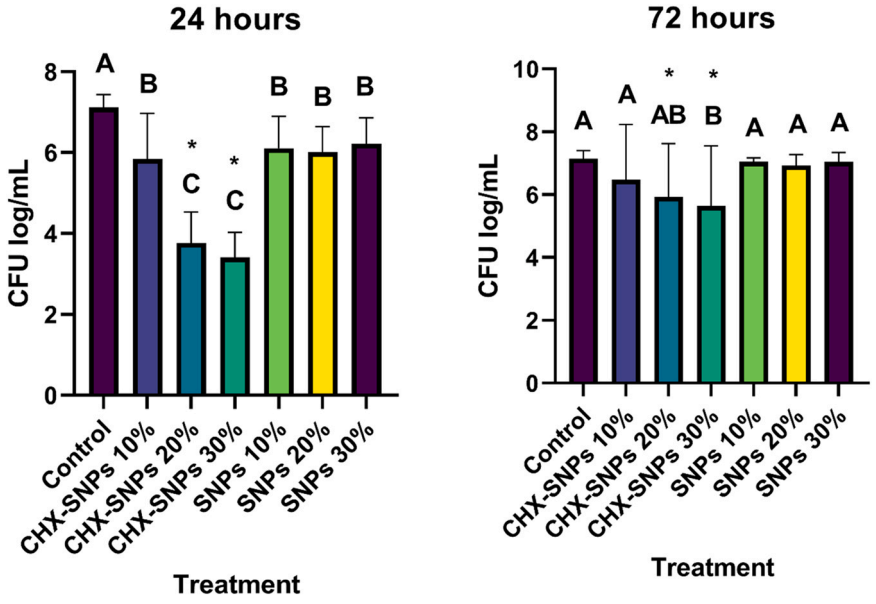

Fig. 7. Means and standard deviations obtained in the biofilm inhibition assays. Mean values followed by the same letter are statistically similar ($p > 0.05$, Two-Way ANOVA/Tukey's test). * indicate statistical differences between the groups for the two.

regardless of the addition of SNPs or CHX-SNPs. It is suggested that the higher the degree of conversion of the polymer matrix, the greater the mechanical strength presented by the experimental composites and, consequently, greater clinical performance [26].

Proportionally to the increase in the degree of conversion, there are also increases of other physicochemical properties [26,27]. Although the groups did not differ statistically from each other in terms of the degree of conversion, higher values of post-gel volumetric shrinkage and flexural strength (after 24 h of light curing) were observed for the CHX-SNPs groups. The modulus of elasticity was significantly higher for the 30% CHX-SNPs group, even after 60 days of immersion in water.

The post-gel volumetric shrinkage results for the SNPs groups, compared to the control group, supported the notion that an increase of inorganic filler particles in composites reduces the polymerization shrinkage [28]. Therefore, for the CHX-SNPs groups, it was assumed that CHX could increase the intermolecular interactions between the monomers during the photopolymerization of the nanocomposite, accelerating this reaction and, consequently, resulting in greater volumetric deformation. This characteristic is not desirable for a restorative material, since the amount of stress at the tooth/material interface, generated by polymerization shrinkage, can cause the adhesive system to rupture, leading to undesired clinical consequences such as fissures and secondary caries [26].

For flexural strength, the particle content was not significant in the groups with CHX (after 24 h of light curing), but these groups showed a statistical difference when compared with the SNPs and control groups. This suggested that experimental composites with CHX-SNPs may be more resistant to cohesive fracture. It should be noted that the results obtained here were below the requirement of the ISO 4049/2000 standard (≥ 80 MPa) [29], probably due to the low concentration of filler particles incorporated into the experimental material. On the other hand, the filler particles were statistically significant for the modulus of elasticity. The composites with 30% SNPs and CHX-SNPs showed higher values for this variable 24 h after light curing, which was consistent with the suggestion that higher modulus proportionally reflects a higher content of inorganic filler particles in the restorative material [26,30].

For some groups, the flexural strength and elastic modulus were influenced by the period during which the specimens were immersed in distilled water, showing an increase or decrease for these properties, depending on the group. This could be explained by the ability of the experimental composite to absorb water, which leads to plasticization, weakening of the three-dimensional polymeric network, and, in the long term, hydrolytic degradation of the organic matrix. This degradation increases the solubility and absorption of more fluids, consequently further weakening the mechanical properties [31–33]. According to Van Landuyt et al. [34], water solubility and sorption are influenced by the level of residual monomers and, consequently, by degradation. Despite the good degree of conversion results for all groups, this hypothesis could not be excluded. For the modulus of elasticity, only the groups with 10% NPs were influenced by the storage time, so it could be speculated that these results may have been related to the low content of nanoparticles incorporated into the experimental composite. On the other hand, for the flexural strength, it was not possible to make this association, because the 30% CHX-SNPs group was influenced by the storage time.

For all the groups, increasing the concentration of filler particles led to a gradual increase in surface roughness. However, despite this increase, no group presented values higher than the critical limit of 0.2 μm [32,35], suggesting that there was no influence of surface roughness on adhesion and accumulation of bacteria on the surfaces of the experimental composites. This could be observed for the SNPs groups, where, despite the increase in surface roughness, there was no difference between the SNPs concentrations in terms of biofilm formation, at both 24 h and 72 h.

Considering the complexity and dynamism of the oral symbiotic microbiome, in addition to outstanding physicochemical properties, it is desirable that dental materials have the potential to combat the accumulation and proliferation of cariogenic bacteria at the limits of dental restoration. The antimicrobial activity of the experimental composites was investigated in bacteria of the genus *Streptococcus*, primary colonizers of the oral biofilm, which make up 60–80% of all bacteria in the first hours of formation [36–38]. The addition of CHX-SNPs in the experimental composite resulted in a restorative material with increased antimicrobial properties, compared to the control and SNPs groups. The antimicrobial activities presented by the nanocomposites were dependent on the concentration of CHX-SNPs, the bacterial species, and, for the biofilms, the time of analysis.

For the inhibition halo, only composites containing CHX-SNPs showed antimicrobial activity, with the antimicrobial performance of the nanocomposites improving as the concentration of CHX-SNPs was increased. These findings suggest that CHX was released from the

restorative material and diffused into the agar medium, significantly inhibiting the growth of all bacteria evaluated around the specimen. Considering the degree of conversion of the groups with CHX, as well as the absence of formation of zones of inhibition for the control and SNPs groups, the hypothesis that bacterial inhibition was due to the accumulation of residual cytotoxic monomers could be excluded. Furthermore, the diffusion of CHX from the nanocomposites confirmed the effective deposition of polyelectrolytes and CHX on the surface of functionalized SNPs, as described by Al Thaher et al. [11], enabling use of the LbL system as a drug nanocarrier.

In addition to antimicrobial action, CHX also has broad-spectrum antibiofilm activity [39]. The antibiofilm efficacy of materials is highly dependent on the time that the antimicrobial remains in the material and, consequently, on its release rate. Therefore, a significant reduction in drug release exposes the surfaces of restorations to colonization by cariogenic bacteria [6].

According to the literature, SNPs and the LbL system act as a reservoir of substances and enable their controlled and sustained release [40–42]. In this study, there was a notable reduction in formation of the *S. mutans* biofilm when the CHX-SNPs was added to the nanocomposites, especially at 30%, at times of 24 h and 72 h, with the most significant effect observed at 24 h, as shown by a greater reduction of CFU/mL. Based on the characteristics of the nanoparticles studied, it was expected that the nanocomposites with CHX-SNPs would present similar inhibition profiles of *S. mutans* biofilm formation at 24 h and 72 h. It is possible that the release of CHX from the nanocomposites decreased over time, due to the depletion of the components of the outer layer. Furthermore, reduced antimicrobial efficacy may be caused by the internal entrapment of CHX-SNPs in the polymeric network formed after the photopolymerization process. Therefore, in the absence of surface CHX-SNPs, *S. mutans* was able to adhere to the surface of the experimental material and form a biofilm within 72 h. Another hypothesis is that over time, the biofilm becomes more structured and thicker, so that the upper layers do not have contact with the restorative material, limiting the antibiofilm action of CHX.

Adverse local and systemic consequences to chlorhexidine have been reported against various eukaryotes in dose and time dependent manner [43–46]; for example chlorhexidine at a concentration of 0.2% was shown to be cytotoxic against human osteoblasts and gingival fibroblasts [47]. In this work, the concentrations of chlorhexidine released after the first day was ~30 μg/mL (0.03% w/v %) that is lower compared to the solution tested in above mentioned studies and lower than the concentration from bone cement containing silica releasing nanocarriers where it was shown no impact on osteoblasts metabolisms [7]; moreover titanium implant releasing chlorhexidine at levels comparable with those in the present study showed antibiofilm efficacy and safety in vivo [48].

The investigation of the influence of SNPs loaded with CHX, synthesized by the LbL method, in experimental composites provided useful advances in the application of CHX drug delivery using these materials. However, further studies are needed to evaluate the long-term antimicrobial efficacy against cariogenic bacteria adhesion and biofilm formation on the surface of the restorative material. Furthermore, information is required concerning the long-term influence of CHX-SNPs on the mechanical properties of experimental composites. It would also be desirable to perform other mechanical analyses, in addition to those employed here. Finally, more experiments should be carried out to determine the ideal concentrations of NPs in experimental composites.

5. Conclusion

The incorporation of CHX-SNPs to experimental composites showed interesting and promising results. These results suggest that NPs exhibit desirable antimicrobial potential against the main bacteria related to oral biofilm formation and can act as fillers, in order to assure satisfactory physicochemical properties of the nanomaterial, modifications and further studies may be required. Therefore, this initial study is the gateway to the synthesis of experimental composites with improved performance using CHX-SNPs.

Acknowledgments

The authors would like to acknowledge the following agencies: São Paulo Research Foundation (FAPESP) (grant# 2019/09010-5), Support Fund for Teaching, Research and Extension – FAEPEX – University of Campinas (grant #2393/19), National Council for Scientific and Technological Development (CNPq), and the Coordination for Improvement of Higher-Level Personnel (CAPES). Prokopovich group would also like to acknowledge SPRINT FAPESP Project 2019/1019-5 and CNPq Project (number: 132616/2020-3) and her personal fellowship by CONFAP - CNPq - The UK Academies 2018.

References

[1] Manzano M, Vallet-Regí M. Mesoporous silica nanoparticles in nanomedicine applications. J Mater Sci Mater Med 2018;29(5):65. https://doi.org/10.1007/s10856-018-6069-x
[2] Jandt KD, Watts DC. Nanotechnology in dentistry: present and future perspectives on dental nanomaterials. Dent Mater 2020;36(11):1365–78.
[3] Boaro LCC, Campos LM, Varca GHC, dos Santos TMR, Marques PA, Sugii MM, et al. Antibacterial resin-based composite containing chlorhexidine for dental applications. Dent Mater 2019;35(6):909–18. https://doi.org/10.1016/j.dental.2019.03.004
[4] Belibasakis GN, Bostanci N, Marsh PD, Zaura E. Applications of the oral microbiome in personalized dentistry. Arch Oral Biol 2019;104:7–12. https://doi.org/10.1016/j.archoralbio.2019.05.023
[5] Raszewski Z, Nowakowska-Toporowska A, Weżgowiec J, Nowakowska D. Design and characteristics of new experimental chlorhexidine dental gels with anti-staining properties. Adv Clin Exp Med 2019;28(7):885–90. https://doi.org/10.17219/acem/94152
[6] Zhang JF, Wu R, Fan Y, Liao S, Wang Y, Wen ZT, et al. Antibacterial dental composites with chlorhexidine and mesoporous silica. J Dent Res 2014;93(12):1283–9. https://doi.org/10.1177/0022034514555143
[7] Al Thaher Y, Alotaibi HF, Yang L, Prokopovich P. PMMA bone cement containing long releasing silica-based chlorhexidine nanocarriers. PLOS ONE 2021;16(9):e0257947https://doi.org/10.1371/journal.pone.0257947
[8] Al Thaher Y, Yang L, Jones SA, Perni S, Prokopovich P. LbL-assembled gentamicin delivery system for PMMA bone cements to prolong antimicrobial activity. PLOS ONE 2018;13(12):e0207753https://doi.org/10.1371/journal.pone.0207753
[9] Perni S, Alotaibi HF, Yergeshov AA, Dang T, Abdullin TI, Prokopovich P. Long acting anti-infection constructs on titanium. J Control Release 2020;326:91–105. https://doi.org/10.1016/j.jconrel.2020.06.013
[10] Perni S, Caserta S, Pasquino R, Jones SA, Prokopovich P. Prolonged antimicrobial activity of PMMA bone cement with embedded gentamicin-releasing silica nanocarriers. ACS Appl Bio Mater 2019;2(5):1850–61. https://doi.org/10.1021/acsabm.8b00752
[11] Al-Thaher Y, Latanza S, Perni S, Prokopovich P. Role of poly-beta-amino-esters hydrolysis and electrostatic attraction in gentamicin release from layer-by-layer coatings. J Colloid Interface Sci 2018;526:35.
[12] Stöber W, Fink A, Bohn E. Controlled growth of monodisperse silica spheres in the micron size range. J Colloid Interface Sci 1968;26(1):62–9.
[13] Muench A, Correa IC, Miranda Grande RH, João M. The effect of specimen dimensions on the flexural strength of a composite resin. J Appl Oral Sci 2005;13(3):265–8.
[14] Tantbirojn D, Chongvisal S, Augustson DG, Versluis A. Hardness and postgel shrinkage of preheated composites. Quintessence Int 2011;42(3):e51–9.
[15] Sakaguchi RL, Versluis A, Douglas WH. Analysis of strain gage method for measurement of post-gel shrinkage in resin composites. Dent Mater 1997;13(4):233–9. https://doi.org/10.1016/s0109-5641(97)80034-6
[16] Boaro LC, Gonçalves F, Guimarães TC, Ferracane JL, Versluis A, Braga RR. Polymerization stress, shrinkage and elastic modulus of current low-shrinkage restorative composites. Dent Mater 2010;26(12):1144–50. https://doi.org/10.1016/j.dental.2010.08.003
[17] Wikler MA, Clinical Editors. Methods for dilution antimicrobial susceptibility tests for bacteria that grow aerobically: approved standard. 2006.
[18] Bai X, Lin C, Wang Y, Ma J, Wang X, Yao X, et al. Preparation of Zn doped mesoporous silica nanoparticles (Zn-MSNs) for the improvement of mechanical and antibacterial properties of dental resin composites. Dent Mater 2020;36(6):794–807. https://doi.org/10.1016/j.dental.2020.03.026
[19] Veloso SRM, Lemos CAA, de Moraes SLD, do Egito Vasconcelos BC, Pellizzer EP, de Melo Monteiro GQ. Clinical performance of bulk-fill and conventional resin composite restorations in posterior teeth: a systematic review and meta-analysis. Clin Oral Investig 2019;23(1):221–33. https://doi.org/10.1007/s00784-018-2429-7
[20] Liu Y, Li Y, Keskin D, Shi L. Poly(β-amino esters): synthesis, formulations, and their biomedical applications. Adv Health Mater 2019;8(2):e1801359https://doi.org/10.1002/adhm.201801359

[21] Iqbal S, Qu Y, Dong Z, Zhao J, Rauf Khan A, Rehman S, et al. Poly (β-amino esters) based potential drug delivery and targeting polymer; an overview and perspectives (review. Eur Polym J 2020;141:110097https://doi.org/10.1016/j.eurpolymj.2020.110097
[22] Karlsson J, Rhodes KR, Green JJ, Tzeng SY. Poly(beta-amino ester)s as gene delivery vehicles: challenges and opportunities. Expert Opin Drug Deliv 2020;17(10):1395–410. https://doi.org/10.1080/17425247.2020.1796628
[23] Wood KC, Boedicker JQ, Lynn DM, Hammond PT. Tunable drug release from hydrolytically degradable layer-by-layer thin films. Langmuir 2005;21(4):1603–9. https://doi.org/10.1021/la0476480
[24] Vázquez E, Dewitt DM, Hammond PT, Lynn DM. Construction of hydrolytically-degradable thin films via layer-by-layer deposition of degradable polyelectrolytes. J Am Chem Soc 2002;124(47):13992–3. https://doi.org/10.1021/ja026405w
[25] Rivera MC, Perni S, Sloan A, Prokopovich P. Anti-inflammatory drug-eluting implant model system to prevent wear particle-induced periprosthetic osteolysis. Int J Nanomed 2019;14:1069–84. https://doi.org/10.2147/IJN.S188193
[26] Cunha DA, Rodrigues NS, Souza LC, Lomonaco D, Rodrigues FP, Degrazia FW, et al. Physicochemical and microbiological assessment of an experimental composite doped with triclosan-loaded halloysite nanotubes. Materials 2018;11(7) [E1080 p.]. Available from. 〈http://europepmc.org/abstract/MED/29941832〉.
[27] Braga RR, Ballester RY, Ferracane JL. Factors involved in the development of polymerization shrinkage stress in resin-composites: a systematic review. Dent Mater 2005;21(10):962–70. https://doi.org/10.1016/j.dental.2005.04.018
[28] Al Sunbul H, Silikas N, Watts DC. Polymerization shrinkage kinetics and shrinkage-stress in dental resin-composites. Dent Mater 2016;32(8):998–1006. https://doi.org/10.1016/j.dental.2016.05.006
[29] International Organization for Standardization. ISO 4049 dentistry — polymer-based filling, restorative and luting materials; 2009. Available from: 〈https://www.iso.org/standard/23041.html〉.
[30] Labella R, Lambrechts P, Van Meerbeek B, Vanherle G. Polymerization shrinkage and elasticity of flowable composites and filled adhesives. Dent Mater 1999;15(2):128–37. https://doi.org/10.1016/s0109-5641(99)00022-6
[31] Ferracane JL. Hygroscopic and hydrolytic effects in dental polymer networks. Dent Mater 2006;22(3):211–22. https://doi.org/10.1016/j.dental.2005.05.005
[32] Rummani G, Ide K, Hosaka K, Tichy A, Abdou A, Otsuki M, et al. Regional ultimate tensile strength and water sorption/solubility of bulk-fill and conventional resin composites: the effect of long-term water storage. Dent Mater J 2021;40(6):1394–402. https://doi.org/10.4012/dmj.2021-101
[33] Nagano D, Nakajima M, Takahashi M, Ikeda M, Hosaka K, Sato K, et al. Effect of water aging of adherend composite on repair bond strength of nanofilled composites. J Adhes Dent 2018;20(5):425–33. https://doi.org/10.3290/j.jad.a41331
[34] Van Landuyt KL, Nawrot T, Geebelen B, De Munck J, Snauwaert J, Yoshihara K, et al. How much do resin-based dental materials release? A meta-analytical approach. Dent Mater 2011;27(8):723–47. https://doi.org/10.1016/j.dental.2011.05.001
[35] Shahminan M, Yap W, Gonzalez MA, Yahya N. Surface roughness of tooth coloured restorative materials. Ann Dent 2020;27:41–9. https://doi.org/10.22452/adum.vol27no7
[36] Samaranayake L, Matsubara VH. Normal oral flora and the oral ecosystem. Dent Clin N Am 2017;61(2):199–215. https://doi.org/10.1016/j.cden.2016.11.002
[37] Huang R, Li M, Gregory RL. Bacterial interactions in dental biofilm. Virulence 2011;2(5):435–44. https://doi.org/10.4161/viru.2.5.16140
[38] Koo H, Falsetta ML, Klein MI. The exopolysaccharide matrix: a virulence determinant of cariogenic biofilm. J Dent Res 2013;92(12):1065–73. https://doi.org/10.1177/0022034513504218. PubMed PMID: 24045647; PubMed Central PMCID: PMCPMC3834652.
[39] Reda B, Hollemeyer K, Trautmann S, Hannig M, Volmer DA. Determination of chlorhexidine retention in different oral sites using matrix-assisted laser desorption/ionization-time of flight mass spectrometry. Arch Oral Biol 2020;110:104623https://doi.org/10.1016/j.archoralbio.2019.104623
[40] Priyadarsini S, Mukherjee S, Mishra M. Nanoparticles used in dentistry: a review. J Oral Biol Craniofac Res 2018;8(1):58–67. https://doi.org/10.1016/j.jobcr.2017.12.004. PubMed PMID: 29556466; PubMed Central PMCID: PMCPMC5854556.
[41] Perni S, Martini-Gilching K, Prokopovich P. Controlling release kinetics of gentamicin from silica nano-carriers. Colloids Surf A Physicochem Eng Asp 2018;541:212–21. https://doi.org/10.1016/j.colsurfa.2017.04.063
[42] Hoang Thi TT, Cao VD, Nguyen TNQ, Hoang DT, Ngo VC, Nguyen DH. Functionalized mesoporous silica nanoparticles and biomedical applications. Mater Sci Eng C Mater Biol Appl 2019;99:631–56. https://doi.org/10.1016/j.msec.2019.01.129
[43] Faria G, Cardoso CR, Larson RE, Silva JS, Rossi MA. Chlorhexidine-induced apoptosis or necrosis in L929 fibroblasts: a role for endoplasmic reticulum stress. Toxicol Appl Pharmacol 2009;234(2):256–65. https://doi.org/10.1016/j.taap.2008.10.012
[44] Giannelli M, Chellini F, Margheri M, Tonelli P, Tani A. Effect of chlorhexidine digluconate on different cell types: a molecular and ultrastructural investigation. Toxicol Vitr: Int J Publ Assoc BIBRA 2008;22(2):308–17. https://doi.org/10.1016/j.tiv.2007.09.012
[45] van Meurs SJ, Gawlitta D, Heemstra KA, Poolman RW, Vogely HC, Kruyt MC. Selection of an optimal antiseptic solution for intraoperative irrigation: an in vitro study. J Bone Jt Surg Am Vol 2014;96(4):285–91. https://doi.org/10.2106/jbjs.M.00313
[46] Mariotti AJ, Rumpf DA. Chlorhexidine-induced changes to human gingival fibroblast collagen and non-collagen protein production. J Periodontol 1999;70(12):1443–8. https://doi.org/10.1902/jop.1999.70.12.1443
[47] John G, Becker J, Schwarz F. Effects of taurolidine and chlorhexidine on SaOS-2 cells and human gingival fibroblasts grown on implant surfaces. Int J Oral Maxillofac Implants 2014;29(3):728–34. https://doi.org/10.11607/jomi.2956
[48] Riool M, Dirks AJ, Jaspers V, de Boer L, Loontjens TJ, van der Loos CM, et al. A chlorhexidine-releasing epoxy-based coating on titanium implants prevents Staphylococcus aureus experimental biomaterial-associated infection. Eur Cell Mater 2017;33:143–57. https://doi.org/10.22203/eCM.v033a11